

Microencapsulation and characterization of controlled release intestinal drugs: a critical review

Section S1 Review methods

The initial search of relevant published journal articles and the literature covered all publication periods from Google Scholar, Web of Science, and Science Direct databases. However, most of the relevant publications reviewed were from 2012 to 2024. The keywords used were: “Oral+intestinal drug microcapsules,” “Oral+intestinal sustained-release microcapsules,” “Preparation+intestinal microcapsules,” and “Core-shell+intestinal microcapsules,” common in various MeID studies. After screening and applying inclusion and exclusion criteria, 162 related research articles were obtained for this review (see Prisma Flow Chart in Fig. S1).

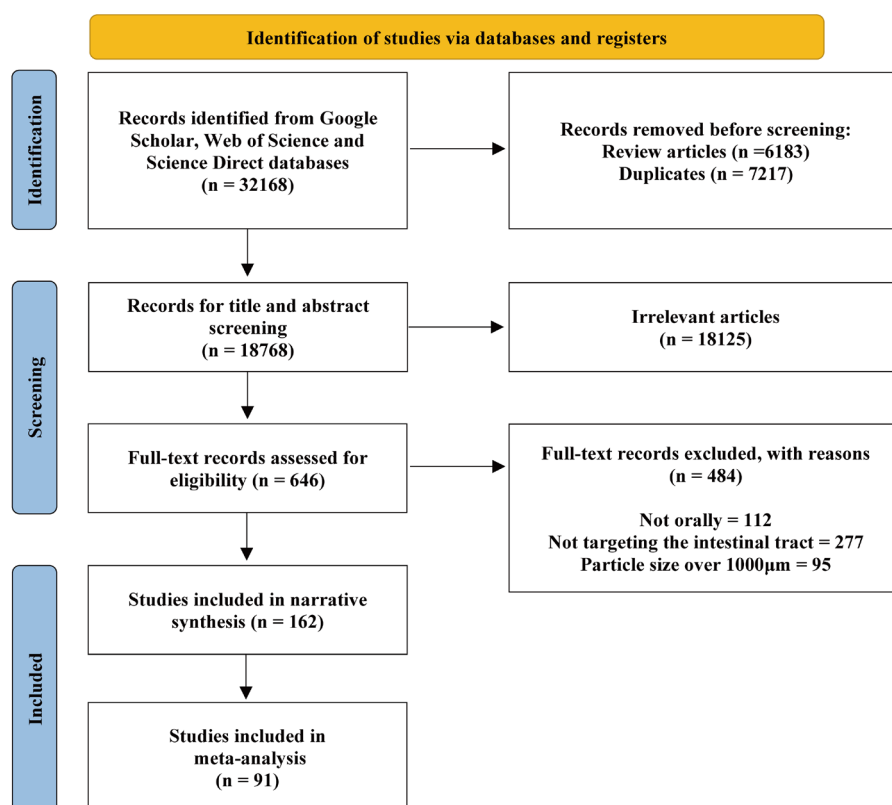


Fig. S1 Prisma process diagram.

Section S2 2D and 3D microfluidic devices

A 2D poly(dimethylsiloxane) (PDMS) microchannel shape can be a T-junction or flow-focusing structure, as shown in Fig. 1f (Shang et al., 2017; Su et al., 2021). Usually, the flow-focusing structure is more commonly used because it is easier to control the droplet size and droplet generation frequency compared to the T-junction structure (Lee et al., 2016). PDMS microfluidic devices have the advantages of flexible design, parallelization, and good reproducibility (Romanowsky et al., 2012; Jo and Lee, 2020). However, they are also limited by swelling in organic solvents, poor hydrophilic and hydrophobic treatments, and complex preparation processes (Lee et al., 2003; Rotem et al., 2012; Samandari et al., 2019). In particular, the hydrophilic and hydrophobic treatments of the PDMS channels are relatively difficult to apply, and can result in the PDMS microfluidic device being unsuitable for the preparation of multiple emulsions (Lee et al., 2016).

The 3D glass capillary microfluidic device shown in Fig. 1e is usually configured by aligning two or more cylindrical capillaries within a square capillary (Choi et al., 2016) in co-flow (same direction) or flow-focusing (opposite direction) configurations (Utada et al., 2007). The droplet diameter in co-flow is larger than the tip diameter, while in the flow-focusing configuration, it is smaller than the aperture size due to the sudden contraction in the aperture generating a high viscous shear force (Jo and Lee, 2020). The surfaces of 3D glass capillary devices can be modified to have hydrophilic or hydrophobic properties in different sections and hence are commonly used for preparing multiple emulsions (Lee et al., 2016; Kim DW et al., 2022). However, they are still manually assembled and difficult to use in the mass production of monodisperse droplets (Lee et al., 2016; Jo and Lee, 2020; Zhang et al., 2022).

Section S3 Double emulsion dispersion methods

Traditional mechanical stirring (Rosca et al., 2004; Huang and Zhou, 2019) needs two emulsification steps (Fig. S2a), but the particle size distribution of the final double emulsion droplets becomes highly polydispersed (Utada et al., 2005). Coaxial electrospray technology can also be used to prepare a double emulsion for functional microcapsules in Fig. S2b (Zhao et al., 2021). Meola et al. (2024) prepared core-shell microcapsules via two-step homogenization and spray drying, with a lipid core that aids in the solubilization and absorption of hydrophobic drugs, and an insulin shell that promotes microbial fermentation to regulate gut microbiota (Fig. S2c). They found that the core-shell microcapsules they prepared with their method reduced the differences in solubility of the drug in fasted and fed states, and increased systemic serotonin concentrations by 2.2 times compared to the pure drug.

Double emulsion microfluidic technology can precisely control the size and number of external and internal droplets to achieve flexible and controllable drug release (Kim JW et al., 2022). For example, Wang X et al. (2022) prepared microcapsules with different wall thicknesses and core numbers using a 3D glass capillary microfluidic device to study drug release properties. Their experimental results showed that single-core microcapsules with uniform wall thickness are conducive to drug encapsulation and controlled release. They found that microcapsules with a wall thickness of 20–30 μm had higher stability and superior release performance in simulated gastric fluid (SGF) and simulated intestinal fluid (SIF) compared to wall thicknesses of 10 or 50 μm (Fig. S2d).

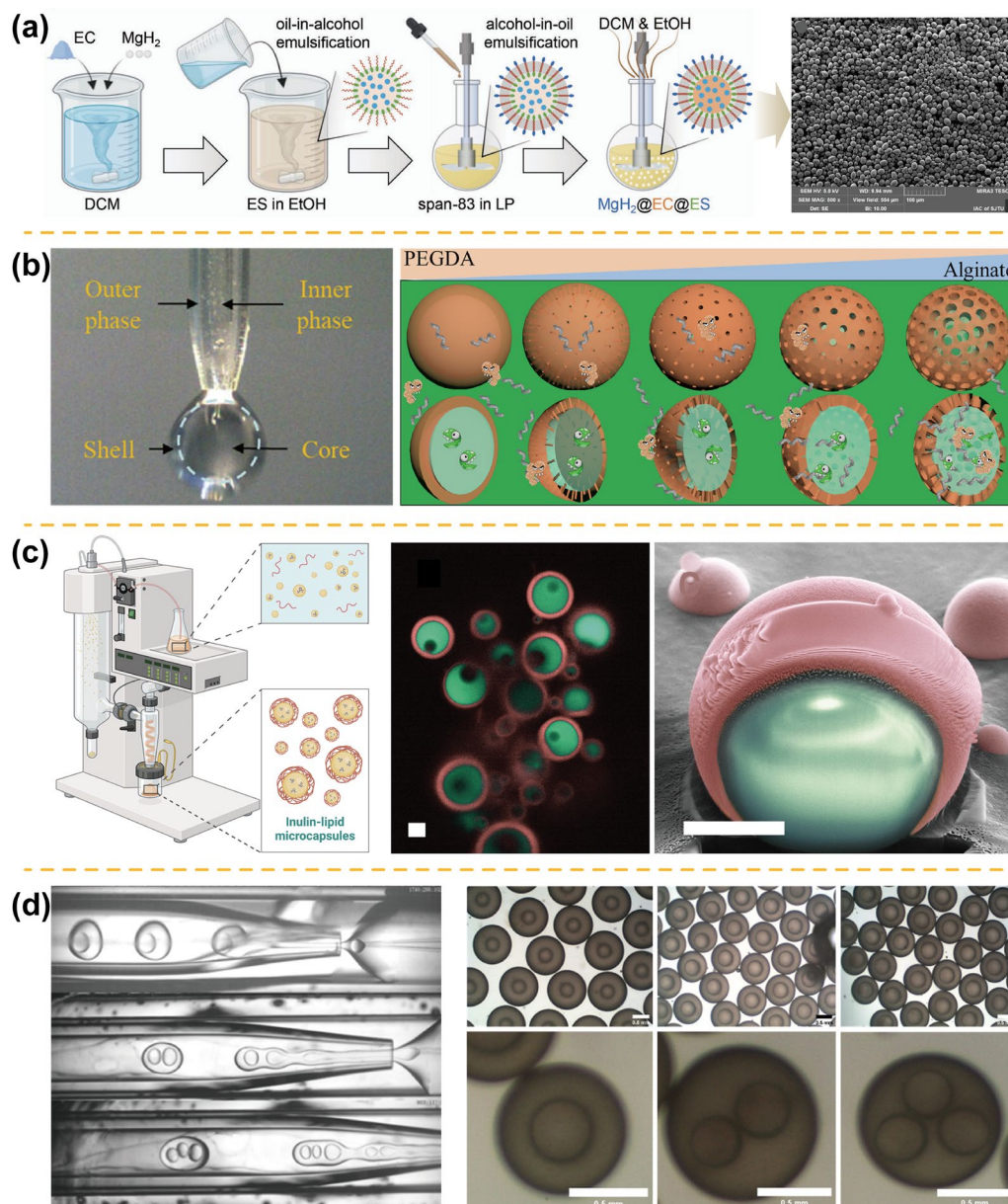


Fig. S2 Preparation of double emulsion droplets. (a) Two-step mechanical stirring. Adapted from Liu H et al. (2024) by permission of John Wiley & Sons. (b) Coaxial electro spray technology. Reprinted from Zhao et al. (2021). (c) Two-step homogenization and spray drying (scale bar=5 μm). Adapted from Meola et al. (2024). (d) Double emulsion 3D capillary microfluidic device (scale bar=0.5 mm). Reprinted from Wang X et al. (2022), Copyright 2022, with permission from Elsevier.

Section S4 Influencing factors of alginate gelation

When sodium alginate is used as the shell material, its performance is influenced by the type of cation, the proportion of G units (α -L-galuronic acid), the crosslinking agent, and the crosslinking temperature (Smidsrod and Skjak-Braek, 1990; Gombotz and Wee, 2012). Jin et al. (2024) studied the properties of microcapsules prepared by sodium alginate and a soy protein isolate with different divalent cations. The results showed that the shrinkage rate of the microcapsules was $\text{Ca}^{2+} > \text{Ba}^{2+} > \text{Cu}^{2+} > \text{Zn}^{2+}$ in SGF at pH=2.0, while the degree of swelling of microcapsules was ranked as $\text{Zn}^{2+} > \text{Ca}^{2+} > \text{Ba}^{2+} > \text{Cu}^{2+}$ in SIF at pH=7.0. Notably, the microcapsules cross-

linked with Zn^{2+} exhibited an initial burst release in the SIF, while the other cations showed a gradual release pattern (Jin et al., 2024). An increase in the proportion of α -L-galuronic acid in sodium alginate results in stronger net gels (Lee and Mooney, 2012; Ramos et al., 2018). In addition, the concentration and duration of the crosslinking agent significantly affect the mechanical strength and drug release mechanism of the microcapsules (Patel et al., 2017; Uyen et al., 2020). Decreasing the crosslinking temperature slows down the crosslinking rate of hydrogels, improves uniformity, and enhances the mechanical properties of the microcapsules (Aguero et al., 2017).

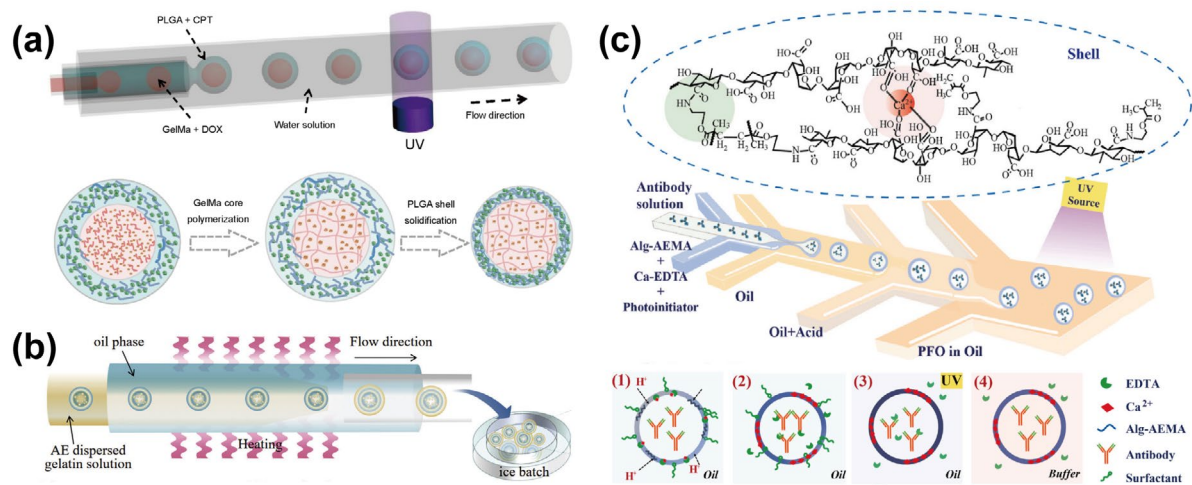
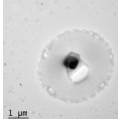
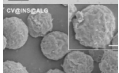
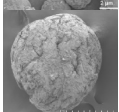


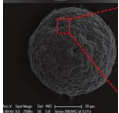
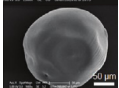
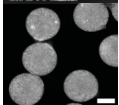
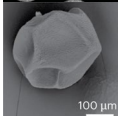
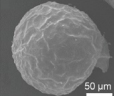
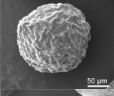
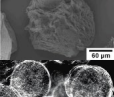
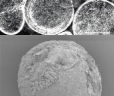
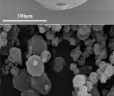
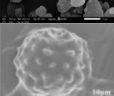
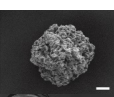
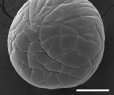
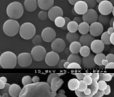
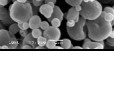

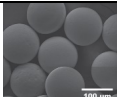
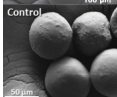
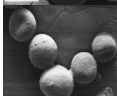
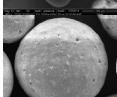
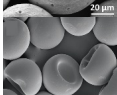
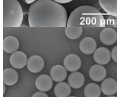
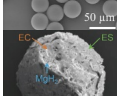
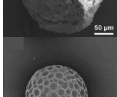
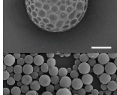
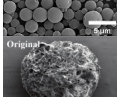



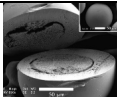
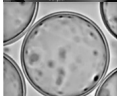
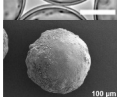
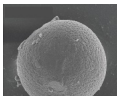
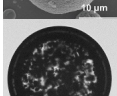
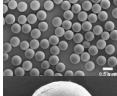
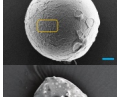
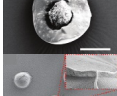
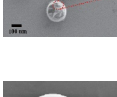
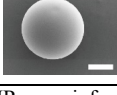
Fig. S3 Other microencapsulation methods. (a) Photopolymerization and solvent evaporation. Reprinted from Li YN et al. (2017). Copyright 2017, with permission from Springer Nature. (b) Ionic crosslinking and freezing. Reprinted from Gan et al. (2022) by permission of John Wiley & Sons. (c) Ionic crosslinking and covalent crosslinking. Reprinted from Li et al. (2022).

Table S1 Preparation methods and characteristics of MeID

Microencapsulation methods	Shell materials	Drugs	Applications	Dispersion methods	Response mechanisms	Coating	Micro/nanocarriers	Morphology	Ref.
Ionic crosslinking	Sodium alginate	Insulin	Diabetes	Mechanical stirring	pH response		Yeast cells		Sabu et al., 2019
	Sodium alginate	Insulin	Diabetes	Mechanical stirring	pH response		Chlorella vulgaris		Ren et al., 2023
	Sodium alginate	Emodin and Tanshinone II A	Renal fibrosis	Extrusion	pH response	Chitosan	PLGA		Sun et al., 2022
	Sodium alginate	Ctx(Ile ²¹)-Ha	Intestinal infections	Extrusion	pH response	HPMCAS and chitosan			Roque-Borda et al., 2023
	Sodium alginate	Bioactive glass	IBD	Extrusion	Enzymatic degradation	Zein protein			Zhu et al., 2023
	Sodium alginate	Methotrexate	Chronic inflammatory diseases	Gas shearing	pH response	Chitosan	Human serum albumin nanoparticles		Zhang et al., 2023
	Sodium alginate	Thiolated hyaluronic acid	IBD	Gas shearing	pH response				Liu et al., 2021
	Sodium alginate	Anti-ICAM	Gastrointestinal pathologies	Gas shearing	pH response	Chitosan	Polystyrene or PLGA		Ghaffarian et al., 2016
	Sodium alginate	Chitosan oligosaccharide	Cholera	Gas shearing	pH response				Liu Y et al., 2024

	Sodium alginate	Selenoprotein	IBD	Electrospray technology	pH response		Hyaluronic acid-modified selenium		Ouyang et al., 2023
	Sodium alginate	Bornyl acetate	Ulcerative colitis	Electrospray technology	pH response		Silk fibroin		Du et al., 2024
	Sodium alginate	Quercetin	High-altitude sleep disturbance	Electrospray technology	pH response	Chitosan-SH	Zein		Wu et al., 2024
	Sodium alginate	Salmonella effector enzyme	IBD	PDMS microfluidic device	pH response	Chitosan	Protein nanoparticles		Ling et al., 2019
	Sodium alginate	Amoxicillin	Drug delivery	L-junction microfluidics	pH and magnetic response	Chitosan	Fe ₃ O ₄ nanoparticles		Yang et al., 2021
	CMI-ZN and CMC-ZN	Docetaxel and atorvastatin	Colorectal cancer	Spray drying	Microbial degradation		Lactoferrin		Elmorshedy et al., 2023
	Sodium alginate and carboxymethylpachyman	<i>Lactiplantibacillus plantarum</i>	Probiotic delivery	Extrusion	pH response		Sporopollenin exine capsules		Deng et al., 2021
	Sodium alginate and resistant starch	Indole-3-propionic acid	Colitis	Electrospray technology	pH response	Chitosan			Yang et al., 2022
	Chitosan	Collagen peptide	Anti-photoaging and antioxidant	Electrospray technology	pH response				Yang et al., 2023
Solvent evaporation	Thioketal polymer	Tacrolimus	Colitis	Mechanical stirring	ROS response				Regmi et al., 2019
	HPMCAS	Insulin	Diabetes	Spray drying	pH response		PLGA		Sun et al., 2016

	HPMCAS	Atorvastatin and celecoxib	Colorectal cancer	Capillary microfluidics	pH response		PSi		Liu et al., 2014
	HPMCAS	Glucagon-like peptide-1	Type 2 diabetes mellitus	Capillary microfluidics	pH response		PLGA or PSi		Araujo et al., 2015
	HPMCAS	Glucagon-like peptide-1	Type 2 diabetes mellitus	Capillary microfluidics	pH response		PLGA		Araujo et al., 2016
	HPMCAS	Atorvastatin and celecoxib	Colon cancer	Capillary microfluidics	pH response		Halloysite nanotubes		Li W et al., 2017
	HPMCAS	Curcumin or dexamethasone	IBD	Capillary microfluidics	pH response		PLGA		Jiang et al., 2021)
	HPMCAS	Fluorouracil and celecoxib	Colorectal cancer	Capillary microfluidics	pH response		PSi		Zhang et al., 2014
	Ethyl cellulose	MgH ₂	IBD	Mechanical stirring	pH response	Eudragit S100		Liu H et al., 2024	
	Ethyl cellulose	Curcumin	Drug delivery	Capillary microfluidics	pH response				Song et al., 2022
	Hydroxyethyl starch	Curcumin and dexamethasone	Ulcerative colitis	Mechanical stirring	Enzyme degradation				Huang et al., 2024
Free radical polymerization	Poly-γ-glutamic acid	Lactobacillus acidophilus	IBD	PDMS microfluidics	NO response				Wang R et al., 2022
	P(AC-co-CL)	Insulin	Diabetes	Capillary microfluidics	pH response				Ma et al., 2023

	PMA and PAM	Ketoprofen and ranitidine HCl	Drug delivery	Capillary microfluidics	pH response				Khan et al., 2015
	PEGDA	Mesenchymal stem cells	Colonic inflammation	Capillary microfluidics	Mechanical stress response				Kim et al., 2022
	Dextran and tannic acid modified with methacrylic acid groups	<i>Escherichia coli</i> Nissle 1917, EcN and indole-3-propionic acid	<i>Ulcerative colitis</i>	Capillary microfluidics	Enzyme degradation				Yang et al., 2024
Freezing	Gelatin	L-Arginine	IBD	Extrusion	Enzyme and microbiota degradation	Polydopamine	Oxidized hyaluronic acid		Fu et al., 2024
	Gelatin	Doxorubicin	Drug delivery	Extrusion	NIR irradiation response	Eudragit L-100	Magnesium-based micromotors		Wu et al., 2019
Ionic crosslinking and solvent evaporation	Sodium alginate and ethyl cellulose	Phycocyanin	Colitis	Capillary microfluidics	pH response				Wang X et al., 2022
Ionic crosslinking and free radical polymerization	Sodium alginate and PEGDA	Alkaline phosphatase	Metabolic syndrome	Electrospray technology	pH response				Zhao et al., 2021
Ionic crosslinking and freezing	Sodium alginate and gelatin	Mesenchymal stem cell-derived exosomes	IBD	Electrospray technology	pH response	Eudragit FS 30D			Gan et al., 2022
Ionic crosslinking and covalent crosslinking	Aminoethylmethacrylate partially functionalized alginate	Infliximab	Colonic inflammation	PDMS microfluidics	pH response				Li et al., 2022
Free radical polymerization and solvent evaporation	Gelatin methacrylate and PLGA	Doxorubicin hydrochloride and camptothecin	Drug delivery	Capillary microfluidics	Biodegradable response				Li YN et al., 2017

CMC: carboxymethyl cellulose; CMI: carboxymethyl inulin; HPMCAS: hypromellose acetate succinate; IBD: inflammatory bowel disease; ICAM: intercellular adhesion molecule; NIR: near-infrared; NO: nitric oxide; PDMS: poly(dimethylsiloxane); PLGA: poly(lactic-co-glycolic acid); PSI: porous silicon; ROS: reactive oxygen species; ZN: zein; P(AC-co-CL): poly(acryloyl carbonate-co-caprolactone); PMA: poly(methyl acrylate); PAM: poly(acrylamide); PEGDA: poly(ethylene glycol) diacrylate.

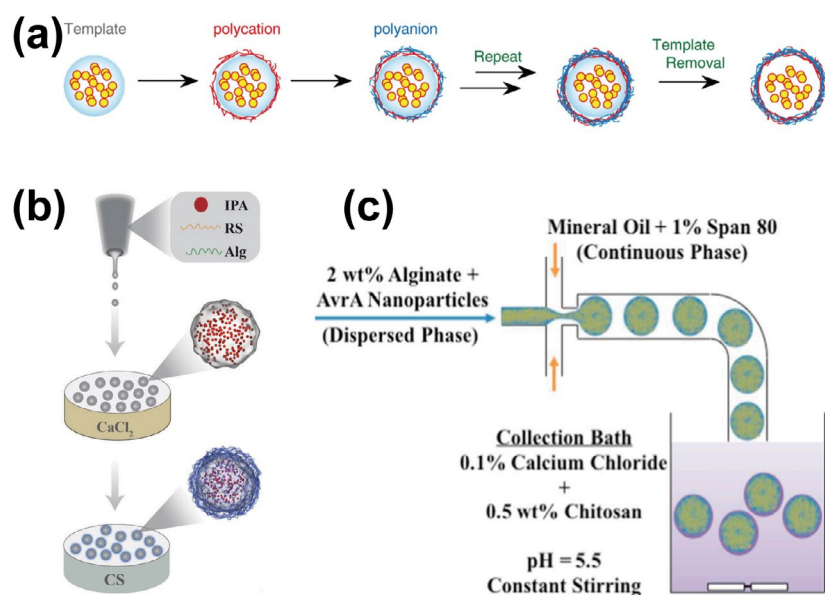


Fig. S4 Coating methods. (a) Coating process. Reprinted from Sato et al. (2011), Copyright 2011, with permission from Elsevier. **(b) Two-step chitosan-coated sodium alginate microcapsules.** Reprinted from Yang et al. (2022). **(c) One-step chitosan-coated sodium alginate microcapsules.** Reprinted from Ling et al. (2019), Copyright 2019, with permission from Elsevier.

Section S5 Micro/nanocarrier applications

Plant pollen shells with porous and hollow structures have been used as drug carriers (Maric et al., 2020; Iravani and Varma, 2021), and coated with enteric materials for delivery to the intestines (Fig. S5a) (Mundargi et al., 2016; Deng et al., 2020).

Ren et al. (2023) used microalgae cells to load insulin and found that through direct release from microalgae and endocytosis by M cells, the insulin entered the bloodstream, with the cellular uptake rate of the insulin microcapsules reaching 88.28% (Fig. S5b).

Jiang et al. (2021) used PLGA nanoparticles to load and encapsulate curcumin and dexamethasone within the shell of microcapsules, and achieved sequential burst-sustained drug release (Fig. S5c).

One drug can be loaded into the nanoparticles as a core, and another can be loaded into the other part of the microcapsules, and the loading ratio of the two drugs can be adjusted (Fig. S5d) (Li W et al., 2017). This method can achieve sequential release (Fig. S5e) (Sun et al., 2022) and enhance the therapeutic effect of combination therapy (Liu et al., 2014).

Zhang et al. (2023) used human serum albumin nanoparticles as drug carriers encapsulated within sodium alginate shell material and found that by exploiting the inflammation-targeting ability, the nanoparticles could be selectively accumulated in inflamed tissues.

Araujo et al. (2015) modified drug carrier PLGA and porous silicon (PSi) nanoparticles and encapsulated them within a shell of hypromellose acetate succinate (HPMCAS) by covalently binding the amino groups of chitosan with the carboxyl groups of cell-penetrating peptides. They found that, compared to unmodified nanoparticles, the interactions of the modified nanoparticles with intestinal cells increased by 5.6-fold (PLGA) and 1.3-fold (PSi) (Fig. S5f).

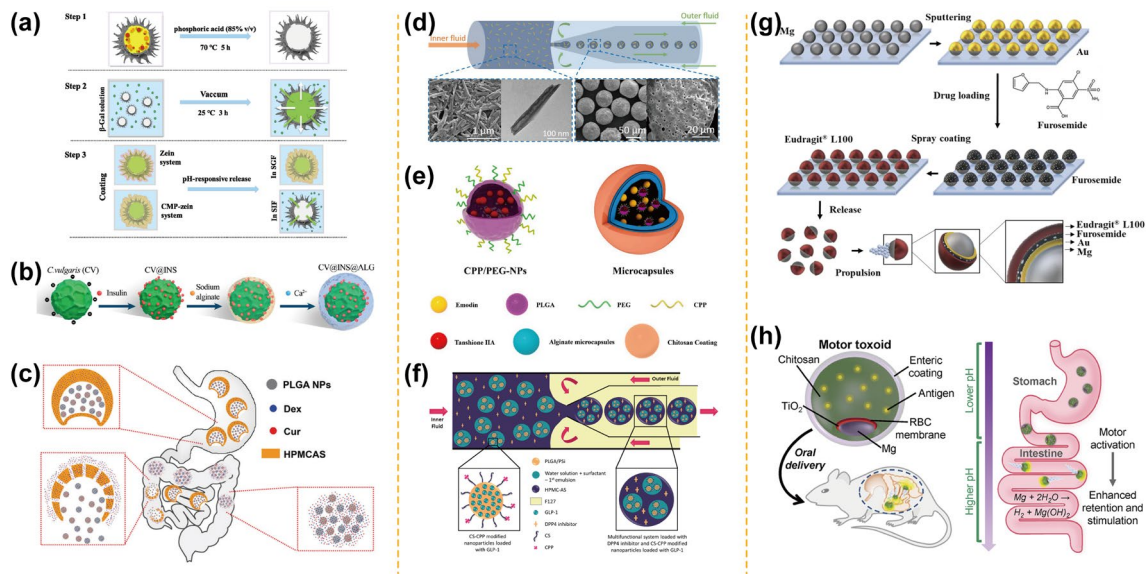


Fig. S5 Micro/nanocarriers in MeID. (a) Pollen shell as a drug carrier. Reprinted from Deng et al. (2020), Copyright 2020, with permission from Elsevier. (b) Microalgae as drug carriers. Reprinted from Ren et al. (2023), Copyright 2023, with permission from the American Chemical Society. (c) Microcapsules with burst-sustained drug release characteristics using poly(lactic-co-glycolic acid) (PLGA) as the drug carrier. Reprinted from Jiang et al. (2021), Copyright 2021, with permission from The Royal Society of Chemistry. (d) Halloysite nanotubes as drug carriers. Reprinted from Li W et al. (2017), Copyright 2017, with permission from Elsevier. (e) Hierarchically structured microcapsules. Reprinted from Sun et al. (2022), Copyright 2022, with permission from Elsevier. (f) Modified PLGA and porous silicon (Psi) nanoparticles achieve dual loading of peptide and enzyme dipeptidyl peptidase 4 inhibitors. Reprinted from AraÚjo et al. (2015), Copyright 2015, with permission from The American Chemical Society. (g) Preparation of magnesium-based micromotor carriers. Reprinted from Maric et al. (2022). (h) Intestinal release of magnesium-based micromotor microcapsules. Reprinted from Wei et al. (2019), Copyright 2019, with permission from the American Chemical Society.

Section S6 Pharmacokinetics and drug release kinetics models

Meola et al. (2024) used spray drying to encapsulate the antipsychotic lurasidone within microcapsules by leveraging a synergistic combination of lipids and inulin. The inulin shell delayed rapid drug release in gastric fluid, while the lipid core not only enhanced lurasidone's solubilization but also, together with its digestion products, inhibited drug recrystallization, thereby increasing its solubility by 2.5 times and oral bioavailability by 8.8 times in the intestine, compared to the pure drug. Yang et al. (2023) prepared high-density, low-porosity microcapsules by crosslinking chitosan with phytic acid, and found from the plot that the microencapsulated drug's peak concentration (C_{max}), the area under the curve (AUC), and peak time (t_{max}) were increased by 1.5-fold, 3.4-fold, and 8-fold, respectively, compared to the drug without encapsulation.

Zero-order kinetics reflect a constant drug release rate and are therefore commonly used in swelling-controlled release microcapsules, such as those with hydrophilic polymers as shell materials (Arifin et al., 2006). First-order kinetics, on the other hand, reflect a decreasing drug release rate over time (Arifin et al., 2006). In diffusion-controlled systems, the Higuchi model is used to describe drug diffusion in a porous spherical matrix, while the Baker-Lonsdale model is suitable for spherical dissolution matrix systems (Arifin et al., 2006). According to experiments by Song et al. (2022), low and high drug-loaded microcapsule drug release at pH 6.8 conforms to the Higuchi model and the zero-order kinetic, respectively, but all microcapsules exhibit first-order kinetic

equation release at pH 7.4. Martinez-Lopez et al. (2019) prepared microcapsules via an extrusion method, using ferulic acid as the shell material and insulin as the encapsulated drug. The dense crosslinked network formed within these microcapsules prevented the penetration of digestive enzymes and was specifically degraded by colonic microbiota. Analysis using the release exponent (n) from the Korsmeyer–Peppas model indicated that different insulin-to-shell material mass ratios (0.06, 0.125, and 0.25) affect the crosslink density and mechanical strength of the microcapsules, thereby influencing drug release kinetics. They found that at a mass ratio of 0.06, high crosslink density and uniform drug distribution resulted in diffusion-controlled release. At a mass ratio of 0.25, low crosslink strength and the formation of large drug aggregates similarly led to diffusion-controlled release. In contrast, microcapsules with a mass ratio of 0.125 exhibited a release mechanism characterized by diffusion-swelling hybrid control due to lower crosslink strength and uniform drug distribution.

Table S2 Mathematic models for drug release kinetics

Model	Equation	Explanation	Application	Ref.
Zero-order kinetics	$\frac{M_t}{M_\infty} = kt$	M_t is the cumulative amount of drug released at time t , M_∞ is the total drug load, and k is the rate constant.	Less swollen matrices or high-molecular weight (MW) polymers	Huang et al., 2008
First order kinetics	$\frac{dC}{dt} = KA(C_s - C)$	Where C is the drug concentration at time t , C_s is the drug solubility, K is the first-order proportional constant, and A is the solid area accessible to dissolution.	Highly swollen matrices or low-MW polymers.	Huang et al., 2008
Higuchi model	$M_t = 4\pi r_0^2 \left[\sqrt{2(C_0 - C_s)C_sDt} + \frac{4C_s D t}{9r_0} \left(\frac{C_s}{2C_0 - C_s} - 3 \right) \right]$	Where M_t , M_∞ , and t are the same as in zero-order kinetics, D is the diffusion coefficient of the drug in the core, C_s is the solubility of the drug in the swollen matrix, C_0 is the initial concentration of the drug, and r_0 is the initial radius of the microsphere.	Porous spherical matrices with dispersed solid drug aggregates.	Arifin et al., 2006; Huang et al., 2008
Baker-Lonsdale model	$\frac{M_t}{M_\infty} = 6\sqrt{\frac{Dt}{\pi r^2}} - \frac{3Dt}{r^2} \quad (0 < M_t/M_\infty < 0.4)$ $\frac{M_t}{M_\infty} = 1 - \frac{6}{\pi^2} \exp\left(-\frac{\pi^2 Dt}{r^2}\right) \quad (0.6 < M_t/M_\infty < 1)$	Where M_t , M_∞ , and t are the same as in zero-order kinetics, D is the diffusion coefficient of the drug in the polymer, and r is the average radius of the spheres.	Drug release from homogeneous spherical matrices, and the drug is in a molecularly dispersed state.	Arifin et al., 2006; Huang et al., 2008
Korsmeyer-Peppas model	$\frac{M_t}{M_\infty} = kt^n$	Where M_t , M_∞ , and t are the same as in zero-order kinetics, k is a constant that incorporates structural and geometric characteristics of the device, and n is the release exponent indicating the mechanism of drug release.	Description of drug release from swelling-controlled systems.	Arifin et al., 2006; Huang et al., 2008; Siepmann and Peppas, 2012; Paarakh et al., 2018
Hopfenberg model	$\frac{M_t}{M_\infty} = 1 - \left(1 - \frac{k_0 t}{C_0 a}\right)^3$	Where M_t , M_∞ , and t are the same as in zero-order kinetics, k_0 is a rate constant, C_0 is a uniform initial drug concentration within the system, and a is the radius of a cylinder or sphere or the half-thickness of a slab.	To describe erosion-controlled drug release from erodible plates, cylinders, and spheres.	Arifin et al., 2006; Huang et al., 2008; Trucillo, 2022

References

- Aguero L, Zaldivar-Silva D, Pena L, et al., 2017. Alginate microparticles as oral colon drug delivery device: a review. *Carbohydr Polym*, 168:32-43. <https://doi.org/10.1016/j.carbpol.2017.03.033>
- Araujo F, Shrestha N, Shahbazi MA, et al., 2015. Microfluidic assembly of a multifunctional tailorable composite system designed for site specific combined oral delivery of peptide drugs. *ACS Nano*, 9(8):8291-8302. <https://doi.org/10.1021/acsnano.5b02762>
- Araujo F, Shrestha N, Gomes MJ, et al., 2016. In vivo dual-delivery of glucagon like peptide-1 (GLP-1) and dipeptidyl peptidase-4 (DPP4) inhibitor through composites prepared by microfluidics for diabetes therapy. *Nanoscale*, 8(20):10706-10713. <https://doi.org/10.1039/c6nr00294c>
- Arifin DY, Lee LY, Wang CH, 2006. Mathematical modeling and simulation of drug release from microspheres: implications to drug delivery systems. *Adv Drug Deliv Rev*, 58(12-13):1274-1325. <https://doi.org/10.1016/j.addr.2006.09.007>
- Choi CH, Lee H, Abbaspourrad A, et al., 2016. Triple emulsion drops with an ultrathin water layer: high encapsulation efficiency and enhanced cargo retention in microcapsules. *Adv Mater*, 28(17):3340-3344. <https://doi.org/10.1002/adma.201505801>
- Deng Z, Wang S, Zhou B, et al., 2020. Carboxymethylpachymaran-zein coated plant microcapsules-based beta-galactosidase encapsulation system for long-term effective delivery. *Food Res Int*, 128:108867. <https://doi.org/10.1016/j.foodres.2019.108867>
- Deng Z, Li J, Song R, et al., 2021. Carboxymethylpachymaran/alginate gel entrapping of natural pollen capsules for the encapsulation, protection and delivery of probiotics with enhanced viability. *Food Hydrocolloids*, 120:106855. <https://doi.org/10.1016/j.foodhyd.2021.106855>
- Du Y, Jiang Y, Song Y, et al., 2024. Alginate/silk fibroin/Zn²⁺ composite microspheres for site-specific delivery for enhanced ulcerative colitis therapy. *Chem Eng J*, 495:153441. <https://doi.org/10.1016/j.cej.2024.153441>
- Elmorshedy YM, Teleb M, Sallam MA, et al., 2023. Engineered microencapsulated lactoferrin nanoconjugates for oral targeted treatment of colon cancer. *Biomacromolecules*, 24(5):2149-2163. <https://doi.org/10.1021/acs.biomac.3c00037>
- Fu YJ, Zhao X, Wang LY, et al., 2024. A gas therapy strategy for intestinal flora regulation and colitis treatment by nanogel-based multistage no delivery microcapsules. *Adv Mater*, 36(19):2309972. <https://doi.org/10.1002/adma.202309972>
- Gan J, Sun L, Chen G, et al., 2022. Mesenchymal stem cell exosomes encapsulated oral microcapsules for acute colitis treatment. *Adv Healthc Mater*, 11(17):e2201105. <https://doi.org/10.1002/adhm.202201105>
- Ghaffarian R, Herrero EP, Oh H, et al., 2016. Chitosan-alginate microcapsules provide gastric protection and intestinal release of ICAM-1-targeting nanocarriers, enabling GI targeting in vivo. *Adv Funct Mater*, 26(20):3382-3393. <https://doi.org/10.1002/adfm.201600084>
- Gombotz WR, Wee SF, 2012. Protein release from alginate matrices. *Adv Drug Deliver Rev*, 64:194-205. <https://doi.org/10.1016/j.addr.2012.09.007>
- Huang D, Wang Y, Xu C, et al., 2024. Colon-targeted hydroxyethyl starch-curcumin microspheres with high loading capacity ameliorate ulcerative colitis via alleviating oxidative stress, regulating inflammation, and modulating gut microbiota. *Int J Biol Macromol*, 266(Pt 1):131107. <https://doi.org/10.1016/j.ijbiomac.2024.131107>
- Huang HJ, Yuan WK, Chen XD, 2008. Microencapsulation based on emulsification for producing pharmaceutical products: a literature review. *Dev Chem Eng Mineral Process*, 14(3-4):515-544. <https://doi.org/10.1002/apj.5500140318>
- Huang Y, Zhou W, 2019. Microencapsulation of anthocyanins through two-step emulsification and release characteristics during in vitro digestion. *Food Chem*, 278:357-363. <https://doi.org/10.1016/j.foodchem.2018.11.073>
- Iravani S, Varma RS, 2021. Plant pollen grains: a move towards green drug and vaccine delivery systems. *Nanomicro Lett*, 13:128. <https://doi.org/10.1007/s40820-021-00654-y>
- Jiang J, Xiao J, Zhao Z, et al., 2021. One-step prepared nano-in-micro microcapsule delivery vehicle with sequential burst-sustained drug release for the targeted treatment of inflammatory bowel disease. *Mater Chem Front*, 5(16):6027-6040. <https://doi.org/10.1039/d1qm00589h>
- Jin H, Wen J, Wang L, et al., 2024. Synthesis and characterization of ion-induced sodium alginate/soy protein isolate microgels for the controlled release. *Food Chem*, 452:139588. <https://doi.org/10.1016/j.foodchem.2024.139588>
- Jo YK, Lee D, 2020. Biopolymer microparticles prepared by microfluidics for biomedical applications. *Small*,

- 16(9):e1903736. <https://doi.org/10.1002/sml.201903736>
- Khan IU, Stolch L, Serra CA, et al., 2015. Microfluidic conceived pH sensitive core-shell particles for dual drug delivery. *Int J Pharm*, 478(1):78-87. <https://doi.org/10.1016/j.ijpharm.2014.10.010>
- Kim DW, Jeong HS, Kim E, et al., 2022. Oral delivery of stem-cell-loaded hydrogel microcapsules restores gut inflammation and microbiota. *J Control Release*, 347:508-520. <https://doi.org/10.1016/j.jconrel.2022.05.028>
- Kim JW, Han SH, Choi YH, et al., 2022. Recent advances in the microfluidic production of functional microcapsules by multiple-emulsion templating. *Lab Chip*, 22(12):2259-2291. <https://doi.org/10.1039/d2lc00196a>
- Lee JN, Park C, Whitesides GM, 2003. Solvent compatibility of poly (dimethylsiloxane)-based microfluidic devices. *Anal Chem*, 75(23):6544-6554.
- Lee KY, Mooney DJ, 2012. Alginate: properties and biomedical applications. *Prog Polym Sci*, 37(1):106-126. <https://doi.org/10.1016/j.progpolymsci.2011.06.003>
- Lee TY, Choi TM, Shim TS, et al., 2016. Microfluidic production of multiple emulsions and functional microcapsules. *Lab Chip*, 16(18):3415-3440. <https://doi.org/10.1039/c6lc00809g>
- Li B, Li X, Chu X, et al., 2022. Micro-ecology restoration of colonic inflammation by in-situ oral delivery of antibody-laden hydrogel microcapsules. *Bioact Mater*, 15:305-315. <https://doi.org/10.1016/j.bioactmat.2021.12.022>
- Li W, Liu D, Zhang H, et al., 2017. Microfluidic assembly of a nano-in-micro dual drug delivery platform composed of halloysite nanotubes and a pH-responsive polymer for colon cancer therapy. *Acta Biomater*, 48:238-246. <https://doi.org/10.1016/j.actbio.2016.10.042>
- Li YN, Yan D, Fu FF, et al., 2017. Composite core-shell microparticles from microfluidics for synergistic drug delivery. *Sci China Mater*, 60(6):543-553. <https://doi.org/10.1007/s40843-016-5151-6>
- Ling K, Wu H, Neish AS, et al., 2019. Alginate/chitosan microparticles for gastric passage and intestinal release of therapeutic protein nanoparticles. *J Control Release*, 295:174-186. <https://doi.org/10.1016/j.jconrel.2018.12.017>
- Liu D, Zhang H, Herranz-Blanco B, et al., 2014. Microfluidic assembly of monodisperse multistage pH-responsive polymer/porous silicon composites for precisely controlled multi-drug delivery. *Small*, 10(10):2029-2038. <https://doi.org/10.1002/sml.201303740>
- Liu H, Cai Z, Wang F, et al., 2021. Colon-targeted adhesive hydrogel microsphere for regulation of gut immunity and flora. *Adv Sci (Weinh)*, 8(18):e2101619. <https://doi.org/10.1002/advs.202101619>
- Liu H, Chen D, Yang X, et al., 2024. Intestine-targeted controlled hydrogen-releasing MgH₂ microcapsules for improving the mitochondrial metabolism of inflammatory bowel disease. *Adv Funct Mater*, 34(33):2316227. <https://doi.org/10.1002/adfm.202316227>
- Liu Y, Wu J, Liu R, et al., 2024. *Vibrio cholerae* virulence is blocked by chitosan oligosaccharide-mediated inhibition of ChsR activity. *Nat Microbiol*, 9:2909-2922. <https://doi.org/10.1038/s41564-024-01823-6>
- Ma Y, Li Q, Yang J, et al., 2023. Crosslinked zwitterionic microcapsules to overcome gastrointestinal barriers for oral insulin delivery. *Biomater Sci*, 11(3):975-984. <https://doi.org/10.1039/d2bm01606k>
- Maric T, Nasir MZM, Rosli NF, et al., 2020. Microrobots derived from variety plant pollen grains for efficient environmental clean up and as an anti-cancer drug carrier. *Adv Funct Mater*, 30(19):2000112. <https://doi.org/10.1002/adfm.202000112>
- Maric T, Atladóttir S, Thamdrup LHE, et al., 2022. Self-propelled janus micromotors for pH-responsive release of small molecule drug. *Appl Mater Today*, 27:101418. <https://doi.org/10.1016/j.apmt.2022.101418>
- Martinez-Lopez AL, Carvajal-Millan E, Sotelo-Cruz N, et al., 2019. Enzymatically cross-linked arabinoxylan microspheres as oral insulin delivery system. *Int J Biol Macromol*, 126:952-959. <https://doi.org/10.1016/j.ijbiomac.2018.12.192>
- Meola TR, Elz A, Wignall A, et al., 2024. Inulin-lipid core-shell microcapsules target the gut microbiota and mimic the pharmaceutical food effect for improved oral antipsychotic delivery. *Adv Funct Mater*, 34(40):2403914. <https://doi.org/10.1002/adfm.202403914>
- Mundargi RC, Potroz MG, Park S, et al., 2016. Natural sunflower pollen as a drug delivery vehicle. *Small*, 12(9):1167-1173. <https://doi.org/10.1002/sml.201500860>
- Ouyang J, Deng B, Zou B, et al., 2023. Oral hydrogel microbeads-mediated in situ synthesis of selenoproteins for regulating intestinal immunity and microbiota. *J Am Chem Soc*, 145(22):12193-12205. <https://doi.org/10.1021/jacs.3c02179>

- Paarakh MP, Jose PA, Setty C, et al., 2018. Release kinetics—concepts and applications. *IJPRT*, 8(1):12-20.
- Patel MA, Aboughaly MH, Schryer-Praga JV, et al., 2017. The effect of ionotropic gelation residence time on alginate cross-linking and properties. *Carbohydr Polym*, 155:362-371. <https://doi.org/10.1016/j.carbpol.2016.08.095>
- Ramos PE, Silva P, Alario MM, et al., 2018. Effect of alginate molecular weight and m/g ratio in beads properties foreseeing the protection of probiotics. *Food Hydrocolloid*, 77:8-16. <https://doi.org/10.1016/j.foodhyd.2017.08.031>
- Regmi S, Pathak S, Nepal MR, et al., 2019. Inflammation-triggered local drug release ameliorates colitis by inhibiting dendritic cell migration and th1/th17 differentiation. *J Control Release*, 316:138-149. <https://doi.org/10.1016/j.jconrel.2019.11.001>
- Ren C, Zhong D, Qi Y, et al., 2023. Bioinspired pH-responsive microalgal hydrogels for oral insulin delivery with both hypoglycemic and insulin sensitizing effects. *ACS Nano*, 17(14):14161-14175. <https://doi.org/10.1021/acsnano.3c04897>
- Romanowsky MB, Abate AR, Rotem A, et al., 2012. High throughput production of single core double emulsions in a parallelized microfluidic device. *Lab Chip*, 12(4):802-807. <https://doi.org/10.1039/c2lc21033a>
- Roque-Borda CA, Saraiva MMS, Macedo Junior WD, et al., 2023. Chitosan and hpmcas double-coating as protective systems for alginate microparticles loaded with ctx(ile(21))-ha antimicrobial peptide to prevent intestinal infections. *Biomaterials*, 293:121978. <https://doi.org/10.1016/j.biomaterials.2022.121978>
- Rosca ID, Watari F, Uo M, 2004. Microparticle formation and its mechanism in single and double emulsion solvent evaporation. *J Control Release*, 99(2):271-280. <https://doi.org/10.1016/j.jconrel.2004.07.007>
- Rotem A, Abate AR, Utada AS, et al., 2012. Drop formation in non-planar microfluidic devices. *Lab Chip*, 12(21):4263-4268. <https://doi.org/10.1039/c2lc40546f>
- Sabu C, Raghav D, Jijith US, et al., 2019. Bioinspired oral insulin delivery system using yeast microcapsules. *Mater Sci Eng C Mater Biol Appl*, 103:109753. <https://doi.org/10.1016/j.msec.2019.109753>
- Samandari M, Alipanah F, Haghjooy Javanmard S, et al., 2019. One-step wettability patterning of pdms microchannels for generation of monodisperse alginate microbeads by in situ external gelation in double emulsion microdroplets. *Sensor Actuat B Chem*, 291:418-425. <https://doi.org/10.1016/j.snb.2019.04.100>
- Sato K, Yoshida K, Takahashi S, et al., 2011. Ph- and sugar-sensitive layer-by-layer films and microcapsules for drug delivery. *Adv Drug Deliv Rev*, 63(9):809-821. <https://doi.org/10.1016/j.addr.2011.03.015>
- Shang L, Cheng Y, Zhao Y, 2017. Emerging droplet microfluidics. *Chem Rev*, 117(12):7964-8040. <https://doi.org/10.1021/acs.chemrev.6b00848>
- Siepmann J, Peppas NA, 2012. Modeling of drug release from delivery systems based on hydroxypropyl methylcellulose (hpmc). *Adv Drug Deliv Rev*, 64:163-174.
- Smidsrod O, Skjak-Braek G, 1990. Alginate as immobilization matrix for cells. *Trends Biotechnol*, 8(3):71-78. [https://doi.org/10.1016/0167-7799\(90\)90139-0](https://doi.org/10.1016/0167-7799(90)90139-0)
- Song XC, Yu YL, Yang GY, et al., 2022. One-step emulsification for controllable preparation of ethyl cellulose microcapsules and their sustained release performance. *Colloids Surf B Biointerfaces*, 216:112560. <https://doi.org/10.1016/j.colsurfb.2022.112560>
- Su Y, Zhang B, Sun R, et al., 2021. Plga-based biodegradable microspheres in drug delivery: Recent advances in research and application. *Drug Deliv*, 28(1):1397-1418. <https://doi.org/10.1080/10717544.2021.1938756>
- Sun J, Xu Z, Hou Y, et al., 2022. Hierarchically structured microcapsules for oral delivery of emodin and tanshinone iia to treat renal fibrosis. *Int J Pharm*, 616:121490. <https://doi.org/10.1016/j.ijpharm.2022.121490>
- Sun S, Liang N, Gong X, et al., 2016. Multifunctional composite microcapsules for oral delivery of insulin. *Int J Mol Sci*, 18(1):54. <https://doi.org/10.3390/ijms18010054>
- Trucillo P, 2022. Drug carriers: A review on the most used mathematical models for drug release. *Processes*, 10(6):1094. <https://doi.org/10.3390/pr10061094>
- Utada A, Chu L-Y, Fernandez-Nieves A, et al., 2007. Dripping, jetting, drops, and wetting: The magic of microfluidics. *Mrs Bull*, 32(9):702-708. <https://doi.org/10.1557/mrs2007.145>
- Utada AS, Lorenceau E, Link DR, et al., 2005. Monodisperse double emulsions generated from a microcapillary device. *Science*, 308(5721):537-541. <https://doi.org/10.1126/science.1109164>
- Uyen NTT, Hamid ZaA, Tram NXT, et al., 2020. Fabrication of alginate microspheres for drug delivery: A review. *Int J Biol Macromol*, 153:1035-1046. <https://doi.org/10.1016/j.ijbiomac.2019.10.233>
- Wang R, Guo K, Zhang W, et al., 2022. Poly - γ - glutamic acid microgel - encapsulated probiotics with gastric acid resistance and smart inflammatory factor targeted delivery performance to ameliorate colitis. *Adv Funct Mater*, 32(26):2113034. <https://doi.org/10.1002/adfm.202113034>

- Wang X, Zhu M, Wang K, et al., 2022. Preparation of core-shell microcapsules based on microfluidic technology for the encapsulation, protection and controlled delivery of phycocyanin. *J Drug Deliv Sci Technol*, 72:103361. <https://doi.org/10.1016/j.jddst.2022.103361>
- Wei X, Beltran-Gastelum M, Karshalev E, et al., 2019. Biomimetic micromotor enables active delivery of antigens for oral vaccination. *Nano Lett*, 19(3):1914-1921. <https://doi.org/10.1021/acs.nanolett.8b05051>
- Wu Y, Tang Z, Du S, et al., 2024. Oral quercetin nanoparticles in hydrogel microspheres alleviate high-altitude sleep disturbance based on the gut-brain axis. *Int J Pharm*, 658:124225. <https://doi.org/10.1016/j.ijpharm.2024.124225>
- Wu Z, Li L, Yang Y, et al., 2019. A microrobotic system guided by photoacoustic computed tomography for targeted navigation in intestines in vivo. *Sci Robot*, 4(32):eaax0613. <https://doi.org/10.1126/scirobotics.aax0613>
- Yang D, Gao K, Bai Y, et al., 2021. Microfluidic synthesis of chitosan-coated magnetic alginate microparticles for controlled and sustained drug delivery. *Int J Biol Macromol*, 182:639-647. <https://doi.org/10.1016/j.ijbiomac.2021.04.057>
- Yang K, Wang X, Huang R, et al., 2022. Prebiotics and postbiotics synergistic delivery microcapsules from microfluidics for treating colitis. *Adv Sci (Weinh)*, 9(16):e2104089. <https://doi.org/10.1002/advs.202104089>
- Yang K, Han HS, An SH, et al., 2023. Mucoadhesive chitosan microcapsules for controlled gastrointestinal delivery and oral bioavailability enhancement of low molecular weight peptides. *J Control Release*, 365:422-434. <https://doi.org/10.1016/j.jconrel.2023.10.021>
- Yang X, Nie W, Wang C, et al., 2024. Microfluidic-based multifunctional microspheres for enhanced oral co-delivery of probiotics and postbiotics. *Biomaterials*, 308:122564. <https://doi.org/10.1016/j.biomaterials.2024.122564>
- Zhang F, Du Y, Zheng J, et al., 2023. Oral administration of multistage albumin nanomedicine depots (mands) for targeted efficient alleviation of chronic inflammatory diseases. *Adv Funct Mater*, 33(9):2211644. <https://doi.org/10.1002/adfm.202211644>
- Zhang H, Liu D, Shahbazi MA, et al., 2014. Fabrication of a multifunctional nano-in-micro drug delivery platform by microfluidic templated encapsulation of porous silicon in polymer matrix. *Adv Mater*, 26(26):4497-4503. <https://doi.org/10.1002/adma.201400953>
- Zhang X, Qu Q, Zhou A, et al., 2022. Core-shell microparticles: From rational engineering to diverse applications. *Adv Colloid Interface Sci*, 299:102568. <https://doi.org/10.1016/j.cis.2021.102568>
- Zhao C, Chen G, Wang H, et al., 2021. Bio-inspired intestinal scavenger from microfluidic electrospray for detoxifying lipopolysaccharide. *Bioact Mater*, 6(6):1653-1662. <https://doi.org/10.1016/j.bioactmat.2020.11.017>
- Zhu Y, Wang Y, Xia G, et al., 2023. Oral delivery of bioactive glass-loaded core-shell hydrogel microspheres for effective treatment of inflammatory bowel disease. *Adv Sci (Weinh)*, 10(18):e2207418. <https://doi.org/10.1002/advs.202207418>